Available online at www.sciencedirect.com

ScienceDirect

Nuclear Physics B 940 (2019) 34–53

NUCLEAR PHYSICS B

www.elsevier.com/locate/nuclphysb

Measurement of P_T-weighted Sivers asymmetries in leptoproduction of hadrons

The COMPASS Collaboration

Received 14 September 2018; received in revised form 6 December 2018; accepted 18 December 2018
Available online 27 December 2018
Editor: Valerie Gibson

Abstract

The transverse spin asymmetries measured in semi-inclusive leptoproduction of hadrons, when weighted with the hadron transverse momentum P_T, allow for the extraction of important transverse-momentum-dependent distribution functions. In particular, the weighted Sivers asymmetries provide direct information on the Sivers function, which is a leading-twist distribution that arises from a correlation between the transverse momentum of an unpolarised quark in a transversely polarised nucleon and the spin of the nucleon. Using the high-statistics data collected by the COMPASS Collaboration in 2010 with a transversely polarised proton target, we have evaluated two types of P_T-weighted Sivers asymmetries, which are both proportional to the product of the first transverse moment of the Sivers function and of the fragmentation function. The results are compared to the standard unweighted Sivers asymmetries and used to extract the first transverse moments of the Sivers distributions for u and d quarks.

1. Introduction

The traditional description of the nucleon structure in hard inclusive processes in terms of collinear parton distribution functions, which depend on the parton light-cone momentum fraction x and on a characteristic hard scale Q^2, was recently generalised to take into account the transverse momentum k_T of the parton with respect to the nucleon direction (for reviews, see [1–3]). A complete picture of the nucleon at leading twist requires a total of eight transverse-momentum-dependent distributions (TMDs). They provide important information on the dynamics of the partons in the transverse plane in momentum space. Upon integration over the transverse momentum, three of them reduce to the number density, the helicity and the transversity collinear distributions. The other five TMDs contain prefactors that are sensitive to the

https://doi.org/10.1016/j.nuclphysb.2018.12.024

direction of the quark transverse momentum vector $\boldsymbol{k}_T$, and their contribution to the hadronic tensor vanishes when integrating over $\boldsymbol{k}_T$.

Among the TMDs, an important rôle is played by the Sivers distribution function $f_{1T}^{\perp q}$ [4–7], which for an unpolarised quark of flavour q describes the correlation between its transverse momentum and the transverse polarisation of the nucleon. In semi-inclusive measurements of deep-inelastic scattering (SIDIS) off a transversely polarised nucleon, the Sivers TMD embodies in the cross section a sine modulation on the difference between the azimuthal angle ϕ_h of the produced hadron and that of the target nucleon spin, ϕ_S.

The Sivers effect was experimentally observed in SIDIS using transversely polarised proton targets, first by the HERMES Collaboration [8,9] and then, at higher energy, by the COMPASS Collaboration [10,11]. The COMPASS measurements on the deuteron [12,13] showed asymmetries compatible with zero within the experimental accuracy. More recently, data on pion production off a transversely polarised ^{3}He target were made available by the Hall A Collaboration at JLab [14]. Combined analyses of these measurements [15–25] allowed for extractions of the Sivers functions and of their first transverse moments $f_{1T}^{\perp\,(1)\,q}$:

$$f_{1T}^{\perp\,(1)\,q}(x) = \int d^2\boldsymbol{k}_T \, \frac{k_T^2}{2M^2} \, f_{1T}^{\perp q}(x, k_T^2), \tag{1}$$

which are found to be different from zero, a very important result in TMD physics. In particular, the u and the d distributions turn out to have similar magnitude, but opposite sign. In Eq. (1), M is the target nucleon mass.

While in most phenomenological studies the first transverse moments of the Sivers distributions are extracted by fitting the data using a given functional form for the x dependence of $f_{1T}^{\perp}$, in Ref. [26] a different approach was adopted: the COMPASS measurements on proton and deuteron targets in the same kinematics were used to extract point-by-point the first transverse moments of the Sivers distributions $f_{1T}^{\perp(1)}$ directly from the data by combining the various asymmetries.

The main problem in all extractions performed up to now is that the standard Sivers asymmetries involve transverse-momentum convolutions of TMDs and fragmentation functions, from which the first transverse moments of the Sivers functions can be obtained analytically only by assuming a specific form, typically a Gaussian, for the transverse-momentum dependence of all involved quantities.

Already twenty years ago an alternative method was proposed [27–29] to determine $f_{1T}^{\perp(1)}$ without making any assumption on the functional form of the transverse-momentum dependence, neither for the distribution functions nor for the fragmentation functions. The method, which consists of measuring asymmetries weighted by the measurable transverse momentum P_T of the hadron, was not pursued; the only and still preliminary results came from HERMES [30]. It is worth to mention that the first transverse moment of the Sivers function enters directly in the Burkardt sum rule [31], which allows to constrain the gluon Sivers function using the measured Sivers functions for quarks [22]. Recently, much interest has been dedicated again to the weighted asymmetries (see e.g. [32,33]).

In this paper, we present the first measurements of two types of P_T-weighted Sivers asymmetries performed by the COMPASS collaboration using the high statistics data collected in 2010 with a 160 GeV muon beam impinging on a transversely polarised proton target. The results are compared to the standard unweighted Sivers asymmetries and used to extract the first transverse moments of the Sivers functions for u and d quarks.

2. The Sivers asymmetries

The Sivers asymmetry is associated to a $\sin\Phi_{\rm Siv} \equiv \sin(\phi_h - \phi_S)$ modulation of the SIDIS cross section in a reference frame where the momentum vectors of virtual photon and nucleon are collinear, the z axis is taken along the virtual-photon momentum and the x axis along the lepton transverse momentum. The relevant part of the fully differential cross section is

$$\mathrm{d}\sigma = \mathrm{d}\sigma_U + S_T\,\mathrm{d}\sigma_S\,\sin\Phi_{\rm Siv}, \tag{2}$$

where S_T is the target nucleon polarisation, and $\mathrm{d}\sigma_U$ and $\mathrm{d}\sigma_S$ are the spin-independent and spin-dependent parts of the cross section, respectively. In the standard, i.e. unweighted case, the Sivers asymmetry is defined as

$$A_{\rm Siv} = 2\,\frac{\int \mathrm{d}\Phi_{\rm Siv}\mathrm{d}\phi_h\,\sin\Phi_{\rm Siv}\,\mathrm{d}\sigma}{\int \mathrm{d}\Phi_{\rm Siv}\mathrm{d}\phi_h\,\mathrm{d}\sigma}\,. \tag{3}$$

At leading twist and leading order in QCD, $A_{\rm Siv}$ is given [29,34] in terms of the Sivers function $f_{1T}^{\perp}$ and the transverse-momentum-dependent unpolarised distribution and fragmentation functions f_1 and D_1 by

$$A_{\rm Siv}(x,z,P_T) = \frac{\sum_q e_q^2 x\,\mathscr{C}\left[\frac{\boldsymbol{P}_T\cdot\boldsymbol{k}_T}{MP_T}\,f_{1T}^{\perp\,q}(x,k_T^2)\,D_1^q(z,p_T^2)\right]}{\sum_q e_q^2 x\,\mathscr{C}\left[f_1^q(x,k_T^2)D_1^q(z,p_T^2)\right]}, \tag{4}$$

where the sums are over quark and antiquark flavours, e_q are the quark charges, and the transverse momentum convolutions are given by

$$\begin{aligned}&\mathscr{C}\left[\frac{\boldsymbol{P}_T\cdot\boldsymbol{k}_T}{MP_T}\,f_{1T}^{\perp\,q}\,D_1^q\right]\\ &\quad\equiv \int \mathrm{d}^2\boldsymbol{k}_T \int \mathrm{d}^2\boldsymbol{p}_T\,\delta^2(z\boldsymbol{k}_T+\boldsymbol{p}_T-\boldsymbol{P}_T)\,\frac{\boldsymbol{P}_T\cdot\boldsymbol{k}_T}{MP_T}\,f_{1T}^{\perp\,q}(x,k_T^2)\,D_1^q(z,p_T^2)\,,\end{aligned} \tag{5}$$

and

$$\mathscr{C}\left[f_1^q\,D_1^q\right] \equiv \int \mathrm{d}^2\boldsymbol{k}_T \int \mathrm{d}^2\boldsymbol{p}_T\,\delta^2(z\boldsymbol{k}_T+\boldsymbol{p}_T-\boldsymbol{P}_T)\,f_1^q(x,k_T^2)\,D_1^q(z,p_T^2)\,. \tag{6}$$

In Eqs. (4), (5), (6), z is the fraction of the longitudinal momentum of the fragmenting quark carried by the produced hadron, $\boldsymbol{p}_T$ is the transverse momentum of the produced hadron with respect to the direction of the fragmenting quark momentum. For simplicity, we have omitted the Q^2 dependence of parton distributions, fragmentation functions and Sivers asymmetry.

When integrating over $\boldsymbol{P}_T$, the denominator of Eq. (4) is easily computed yielding the familiar "collinear" expression

$$\sum_q e_q^2 x \int \mathrm{d}^2\boldsymbol{P}_T\,\mathscr{C}\left[f_1^q\,D_1^q\right] = \sum_q e_q^2 x\,f_1^q(x)D_1^q(z)\,, \tag{7}$$

where $f_1^q(x)$ and $D_1^q(z)$ are the above defined partonic functions integrated over the transverse momentum, while, in the general case, the numerator of Eq. (4) cannot be analytically evaluated. Hence, in order to disentangle $f_{1T}^{\perp}$ and D_1 and to extract the Sivers function, some functional form must be assumed for the transverse-momentum dependence of the distribution and fragmentation functions. Assuming this form to be a Gaussian, the Sivers asymmetry becomes [15,16,29]

$$A_{\mathrm{Siv,G}}(x,z) = \frac{a_{\mathrm{G}} \sum_q e_q^2 x f_{1T}^{\perp\,(1)\,q}(x) z D_1^q(z)}{\sum_q e_q^2 x f_1^q(x) D_1^q(z)}\,. \tag{8}$$

The factor a_G in Eq. (8) is

$$a_{\mathrm{G}} = \frac{\sqrt{\pi} M}{\sqrt{\langle p_T^2\rangle + z^2 \langle k_T^2\rangle_S}}\,, \tag{9}$$

where $\langle p_T^2\rangle$ and $\langle k_T^2\rangle_S$ are the Gaussian widths of the fragmentation function and of the Sivers function, respectively. In the Gaussian model, the average transverse momentum of the produced hadrons (integrated over its azimuthal angle) is written as

$$\langle P_T\rangle = \frac{\sqrt{\pi}}{2}\sqrt{\langle p_T^2\rangle + z^2\langle k_T^2\rangle}\,, \tag{10}$$

where $\langle k_T^2\rangle$ is the width of the transverse-momentum-dependent number density f_1, which in principle differs from $\langle k_T^2\rangle_S$. Taking approximately $\langle k_T^2\rangle_S \simeq \langle k_T^2\rangle$, we can write a_{G} as

$$a_{\mathrm{G}} \simeq \frac{\pi M}{2\langle P_T\rangle}. \tag{11}$$

The Gaussian ansatz clearly introduces a bias into the extraction of the Sivers function. In order to avoid this problem one can consider, instead of Eq. (3), an asymmetry that is weighted by the transverse momentum of the produced hadron. In particular, when choosing $w = P_T/zM$ as weight, the weighted Sivers asymmetry becomes

$$A_{\mathrm{Siv}}^{w} = \frac{\int \mathrm{d}\Phi_{\mathrm{Siv}}\, \sin\Phi_{\mathrm{Siv}} \int \mathrm{d}^2\boldsymbol{P}_T \left(\frac{P_T}{zM}\right) \mathrm{d}\sigma}{\int \mathrm{d}\Phi_{\mathrm{Siv}} \int \mathrm{d}^2\boldsymbol{P}_T\, \mathrm{d}\sigma}\,. \tag{12}$$

In terms of quark distribution and fragmentation functions, it reads

$$A_{\mathrm{Siv}}^{w}(x,z) = \frac{\sum_q e_q^2 x \int \mathrm{d}^2\boldsymbol{P}_T \frac{P_T}{zM}\mathscr{C}\left[\frac{\boldsymbol{P}_T\cdot\boldsymbol{k}_T}{MP_T} f_{1T}^{\perp\,q}(x,k_T^2)\, D_1^q(z,p_T^2)\right]}{\sum_q e_q^2 x\, f_1^q(x) D_1^q(z)}. \tag{13}$$

The convolution in the numerator can now be carried out in a straightforward way (see Appendix A) and the final expression is

$$A_{\mathrm{Siv}}^{w}(x,z) = 2\,\frac{\sum_q e_q^2 x f_{1T}^{\perp\,(1)\,q}(x) D_1^q(z)}{\sum_q e_q^2 x f_1^q(x) D_1^q(z)}\,, \tag{14}$$

which shows that the asymmetry contains the product of the first k_T^2 moment of the Sivers function and the unpolarised fragmentation function.

When using $w' = P_T/M$ as weight, the resulting Sivers asymmetry reads

$$A_{\mathrm{Siv}}^{w'} = \frac{\int \mathrm{d}\Phi_{\mathrm{Siv}}\, \sin\Phi_{\mathrm{Siv}} \int \mathrm{d}^2\boldsymbol{P}_T \left(\frac{P_T}{M}\right) \mathrm{d}\sigma}{\int \mathrm{d}\Phi_{\mathrm{Siv}} \int \mathrm{d}^2\boldsymbol{P}_T\, \mathrm{d}\sigma}\,. \tag{15}$$

This asymmetry is of interest because it should exhibit a z dependence close to that of the unweighted asymmetries. Its expression in the parton model,

$$A_{\rm Siv}^{w'}(x,z) = 2\frac{\sum_q e_q^2 x f_{1T}^{\perp\,(1)\,q}(x)\, z D_1^q(z)}{\sum_q e_q^2 x f_1^q(x)\, D_1^q(z)}\,, \tag{16}$$

is indeed very similar to that of the unweighted asymmetry in the Gaussian model, Eq. (8). In particular, from Eqs. (8), (11), (16) one sees that the ratio $A_{\rm Siv}^{w'}/A_{\rm Siv,G}$ is related to the average value of the hadron transverse momentum:

$$\frac{A_{\rm Siv}^{w'}}{A_{\rm Siv,G}} \simeq \frac{4\langle P_T\rangle}{\pi M}\,. \tag{17}$$

From Eqs. (14) and (16) it is clear that the first k_T^2 moment of the Sivers functions can be obtained in a straightforward way from both types of weighted asymmetries. The advantage of the P_T/zM weighting is that the factor z does not appear at the numerator of the Sivers asymmetry, so that the fragmentation functions have the same weight both in numerator and denominator. For this reason, in this work $f_{1T}^{\perp(1)}$ was extracted using $A_{\rm Siv}^{w}$ (see Section 6).

3. Experimental set-up and data analysis

The COMPASS spectrometer [35,36] is in operation in the SPS North Area of CERN since 2002. The data used in this analysis were collected in 2010 by scattering a 160 GeV μ^+ beam on a transversely polarised target. The 1.2 m long NH_3 target was kept at 50 mK in a dilution refrigerator cryostat and segmented in three cells, 30 cm, 60 cm and 30 cm long respectively. The proton polarisation of about 80% was oriented vertically by a 0.63 T magnetic field that was provided by the saddle coils of the polarised target magnet [37]. The data were taken at a mean beam intensity of 3.5×10^8 μ/spill, for a spill length of about 10 s every 40 s. About 37×10^9 events, corresponding to 1.9 PB of data, were collected in twelve separate periods. In order to minimize systematic errors, during each period of data taking the orientation of the proton polarisation in the three target cells was either up–down–up or down–up–down in the first subperiod, and reversed in the second one. By suitably combining the data, instrumental asymmetries could be limited to negligible values. The principles of the measurement and the data analysis were already described in several publications [10–12] and will not be repeated here.

In order to allow for a comparison of the weighted Sivers asymmetries with the unweighted asymmetries, all constraints to select DIS events and final-state hadrons are the same as for the published data [11]. Here we only recall that in order to ensure the DIS regime only events with photon virtuality $Q^2 > 1\ (\mathrm{GeV}/c)^2$, fractional energy of the virtual photon $0.1 < y < 0.9$, and mass of the hadronic final-state system $W > 5\ \mathrm{GeV}/c^2$ are considered. A charged hadron is required to have a transverse momentum $P_T \geq 0.1\ \mathrm{GeV}/c$ and a fraction of the available energy $z > 0.2$. With these constraints, about 8×10^7 hadrons are left and used for the extraction of the asymmetries. This sample consists mainly of pions (about 70% for positive hadrons, 75% for negative hadrons [38]). In addition, the analysis was also done for charged hadrons in the region $0.1 < z < 0.2$.

The weighted asymmetries are measured separately for positive and negative hadrons as a function of x or z. For each bin in x or z and for each period of data taking, the asymmetries are extracted from the number of hadrons produced in each cell for the two directions of the target polarisation, and the mean of the results from the twelve periods is taken as the final result.

The unweighted asymmetries were extracted using both an extended unbinned maximum likelihood method and the so-called double ratio method (DRM). The two methods led to very

similar results and the small differences were added to the systematic uncertainties. In both cases, the hadrons produced in the two data-taking subperiods and in the three target cells are combined in order to ensure cancellation of the azimuthal acceptance and of the beam flux. Since only the counts in the numerator of the expression of $A^w_{\rm Siv}$ are weighted, a modified DRM is used in this analysis.

In each kinematic bin, we divide the $\Phi_{\rm Siv}$ range in 12 bins, and in each of them we calculate the quantity

$$R(\Phi_{\rm Siv}) = \frac{\Delta^w}{\sqrt{\Sigma^w \Sigma}}\,, \tag{18}$$

where

$$\Delta^w = N^w_+ N'^w_+ - N'^w_- N^w_-\,, \quad \Sigma^w = N^w_+ N'^w_+ + N'^w_- N^w_-\,, \quad \Sigma = N_+ N'_+ + N'_- N_-\,. \tag{19}$$

Here N and N^w are the total number of hadrons in that bin and the sum of the weights associated to each hadron, respectively, and N (N') refers to the first (second) subperiod. The numbers of hadrons produced in the first and in the third target cell, which are always polarised in the same direction, are added up. The subscripts $+$ and $-$ indicate the up and down orientation of the target polarisation. Both azimuthal acceptance and beam flux cancel in the ratio of Eq. (18), so that

$$R(\Phi_{\rm Siv}) \simeq 4 \bar{S}_T\, A^w_{\rm Siv}\, \sin\Phi_{\rm Siv}, \tag{20}$$

where $\bar{S}_T$ is the mean transverse polarisation of the target protons. Cancellation of azimuthal acceptance is guaranteed as long as the ratios of the acceptances of the oppositely polarised cells in the two data taking subperiods are the same, which is the so-called "reasonable assumption" [13].

Several tests were performed to assess the correctness of the results and the size of possible systematic uncertainties. Two alternative estimators were used, which are not expected to guarantee an as good cancellation of the azimuthal acceptance as the modified DRM but are much simpler, one of them being the mean value of $\sin\Phi_S\, P_T/zM$. It turned out that the results are essentially identical.

The effect of the P_T/z acceptance was also investigated. This acceptance is about 60% and rather flat in the range $0.020 < x < 0.7$ both for positive and negative hadrons. At smaller x it increases smoothly from 0.4 to about 0.8 as P_T/z increases from 0.1 GeV/c to 10 GeV/c. In order to evaluate the effect of the acceptance in the results, we have re-evaluated $A^w_{\rm Siv}$ after having corrected for the P_T/z acceptance. The difference between the results obtained with and without the corrections is at most one tenth of a standard deviation, and thus negligible.

The stability of the results was checked paying particular attention to the P_T limits. The effect of the lower P_T cut, which is expected to be negligible, was investigated by extracting the weighted Sivers asymmetries using three different lower cuts, $P_T > 0.15$ GeV/c, $P_T > 0.20$ GeV/c and $P_T > 0.25$ GeV/c. Also, the effect of a cut on the upper value of P_T was investigated by extracting the asymmetries using the limits: $P_T < 1.5$ GeV/c, $P_T < 1.25$ GeV/c and $P_T < 1.0$ GeV/c. In all the cases the differences to the results obtained with the standard cuts are negligibly small in all x bins.

The contributions from higher-order processes, i.e. QCD Compton and photon–gluon fusion, which are more relevant at high P_T [39], have neither been taken into account nor corrected for.

Altogether, no evidence was found for additional relevant systematic uncertainties. The systematic uncertainties are estimated to be half of the statistical uncertainties, as in the analysis of the standard Sivers asymmetries of the same data [11].

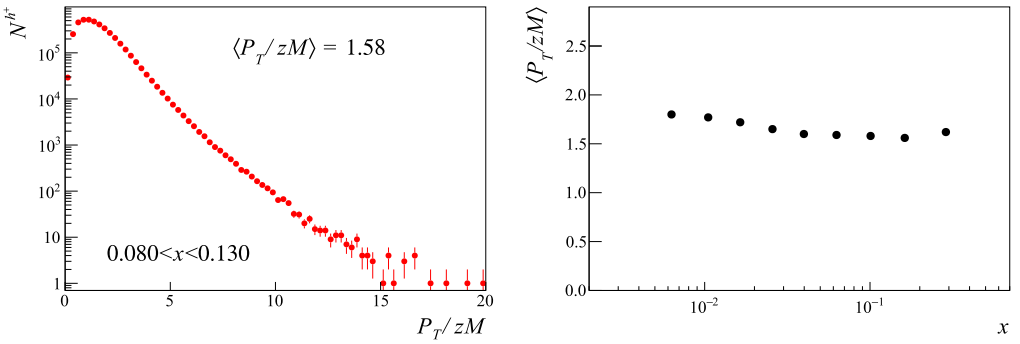

Fig. 1. Left panel: distribution of the weight $w = P_T/zM$ for positive hadrons in the bin $0.080 < x < 0.13$. Right panel: mean value of w as function of x. No acceptance correction applied.

Table 1
Mean values of the weight P_T/zM for positive hadrons in the nine bins of x for $z > 0.2$, and in the nine bins of z.

$\langle x\rangle$	$\langle P_T/zM\rangle$	$\langle z\rangle$	$\langle P_T/zM\rangle$
0.0063	1.80	0.14	3.13
0.0105	1.77	0.22	2.19
0.0164	1.72	0.27	1.88
0.0257	1.65	0.32	1.66
0.0399	1.60	0.37	1.50
0.0629	1.59	0.44	1.32
0.101	1.58	0.57	1.11
0.163	1.56	0.72	0.89
0.288	1.62	0.88	0.63

4. Sivers asymmetries weighted by P_T/zM

The distributions of the weights $w = P_T/zM$ are very similar for all nine x bins. As an example, the distribution for positive hadrons in the bin $0.080 < x < 0.130$ is shown in the left panel of Fig. 1. The mean values of w in the nine x bins are given in the right panel of the same figure and in Table 1. For negative hadrons the distributions are very much the same. The distributions of w in the nine z bins have also similar shapes but different slopes. The distribution for $0.50 < z < 0.65$ and the mean values of w as function of z are shown in Fig. 2 for positive hadrons. Again, for negative hadrons the distributions are very much the same.

The measured weighted asymmetries are presented as a function of x in Fig. 3. The unweighted Sivers asymmetries [11] are also shown for comparison. As expected, the trends of the weighted and unweighted asymmetries are similar both for positive and negative hadrons. The asymmetry for positive hadrons is clearly different from zero, in particular at large x. In this range, the ratios $A^w_{\rm Siv}/A_{\rm Siv}$ for positive hadrons are very close to the mean value of the weight, and the statistical uncertainties are scaled by about the same amount.

Assuming u-quark dominance for positive hadrons produced on a proton target, one has

$$A^w_{\rm Siv} \simeq 2\,\frac{f_{1T}^{\perp(1)u}(x,Q^2)}{f_1^u(x,Q^2)}\,, \tag{21}$$

and the results on $A^w_{\rm Siv}$ represent the first direct measurement of $f_{1T}^{\perp(1)\,u}/f_1^u$.

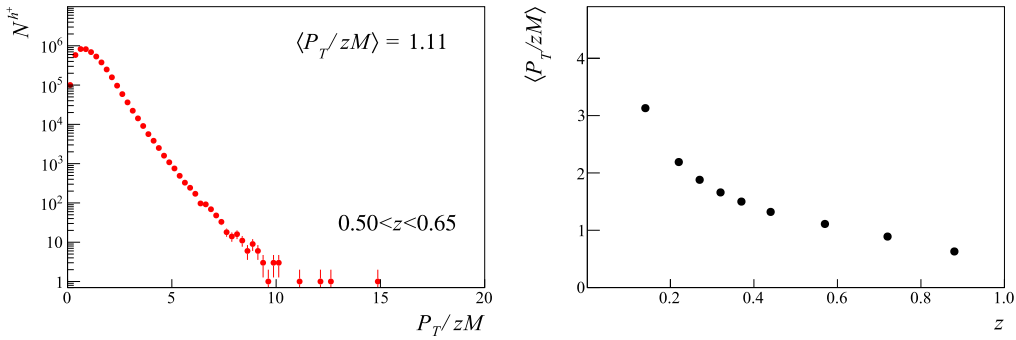

Fig. 2. Left panel: distribution of the weight $w = P_T/zM$ for positive hadrons in the bin $0.50 < z < 0.65$. Right panel: mean value of w as function of z. No acceptance correction applied.

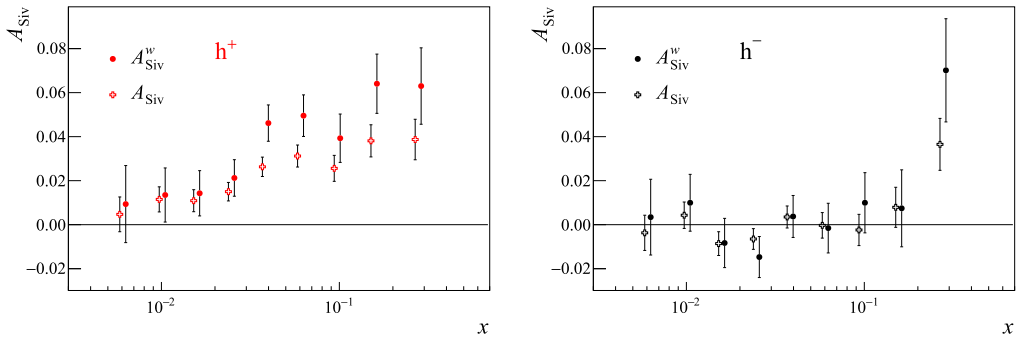

Fig. 3. Full points: $A^w_{\rm Siv}$ in the nine x bins for positive (left panel) and negative (right panel) hadrons. The open crosses are the unweighted Sivers asymmetries $A_{\rm Siv}$ [11], which are slightly shifted towards smaller x values for clarity.

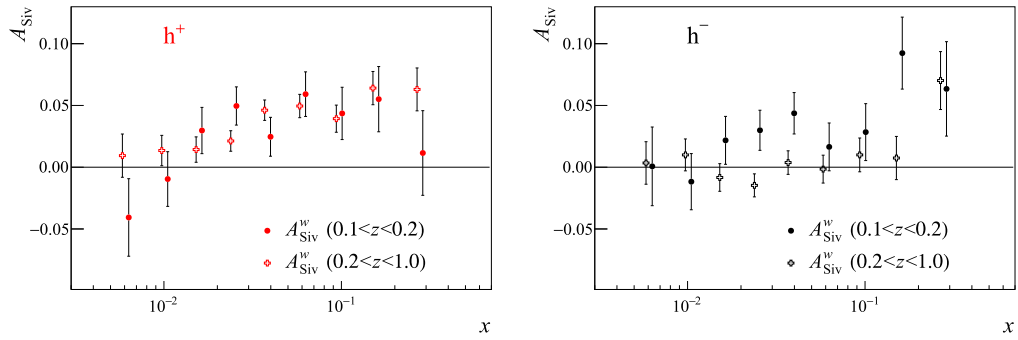

Fig. 4. Comparison of the weighted asymmetries vs. x measured in the range $(0.1 < z < 0.2)$ for positive (left) and negative (right) hadrons and the corresponding ones in the standard range $z > 0.2$, which are slightly shifted towards smaller x values for clarity.

In Fig. 4, the weighted Sivers asymmetries measured in our standard range $z > 0.2$ are compared with the corresponding ones in the range $0.1 < z < 0.2$. It is interesting to note that the positive-hadron asymmetries are basically unchanged, which emphasizes u-quark dominance and supports the idea that factorisation works already at small values of z in the COMPASS kine-

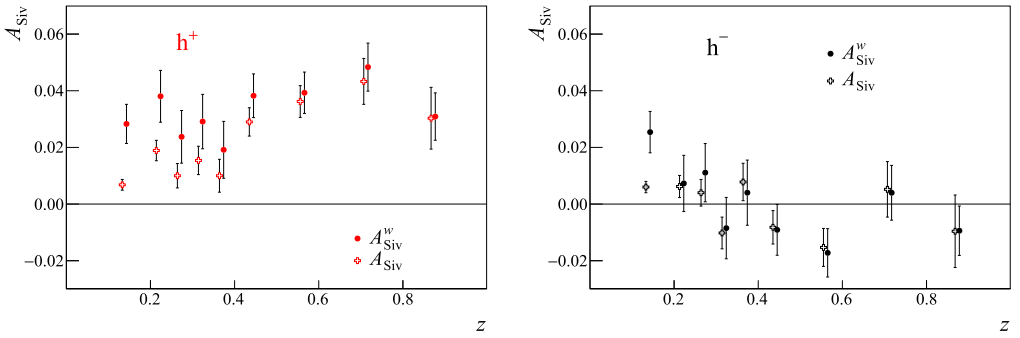

Fig. 5. Full points: $A^w_{\rm Siv}$ in the nine z bins for positive (left panel) and negative (right panel) hadrons. The open crosses are the corresponding unweighted Sivers asymmetries $A_{\rm Siv}$ [11], which are slightly shifted towards smaller x values for clarity.

Table 2
Measured values of the P_T/zM-weighted Sivers asymmetries in the nine x bins.

	$z > 0.2$		$0.1 < z < 0.2$	
x	$A^w_{\rm Siv}$, h^+	$A^w_{\rm Siv}$, h^-	$A^w_{\rm Siv}$, h^+	$A^w_{\rm Siv}$, h^-
0.003–0.008	0.009 ± 0.018	0.003 ± 0.017	-0.041 ± 0.031	0.001 ± 0.032
0.008–0.013	0.013 ± 0.012	0.010 ± 0.013	-0.010 ± 0.022	-0.012 ± 0.023
0.013–0.020	0.014 ± 0.010	-0.008 ± 0.011	0.030 ± 0.019	0.022 ± 0.019
0.020–0.032	0.021 ± 0.008	-0.015 ± 0.009	0.050 ± 0.015	0.030 ± 0.016
0.032–0.050	0.046 ± 0.008	0.004 ± 0.010	0.025 ± 0.016	0.044 ± 0.017
0.050–0.080	0.050 ± 0.009	-0.002 ± 0.011	0.059 ± 0.018	0.016 ± 0.019
0.080–0.130	0.039 ± 0.011	0.010 ± 0.014	0.044 ± 0.021	0.028 ± 0.023
0.130–0.210	0.064 ± 0.013	0.007 ± 0.017	0.055 ± 0.026	0.092 ± 0.029
0.210–0.700	0.063 ± 0.017	0.070 ± 0.023	0.012 ± 0.034	0.063 ± 0.038

matic range. At low z, the difference between favoured and unfavoured fragmentation functions decreases, thus it is expected that the u-quark contribution to the negative-hadron asymmetry increases. The asymmetry itself is then expected to become larger and similar to the positive-hadron asymmetries, as observed in Fig. 4.

In order to further investigate the z dependence, it is of interest to look at $A^w_{\rm Siv}$ as a function of z, after integration over x. The results in the range $0.1 < z < 1$ are shown in Fig. 5. For positive hadrons, the values are almost constant within statistical uncertainties, as it is expected in the case of u-quark dominance if the measurement is performed in the current-fragmentation region and factorisation holds. The values of the measured P_T/zM-weighted asymmetries are given in Tables 2 and 3.

5. Sivers asymmetries weighted by P_T/M

Let us now turn to the Sivers asymmetries weighted with $w' = P_T/M$. The distributions of w' are very similar in all x and z bins. Examples of the distributions and the mean values of w' in the x and z bins for positive hadrons are given in Figs. 6 and 7, respectively, and in Table 4. Again, for negative hadrons the distributions are very much the same.

Table 3
Measured values of the P_T/zM-weighted Sivers asymmetries in the nine z bins.

z	$A^w_{\rm Siv}$, h^+	$A^w_{\rm Siv}$, h^-
0.10−0.20	0.0283 ± 0.0069	0.0254 ± 0.0073
0.20−0.25	0.0380 ± 0.0091	0.0073 ± 0.0099
0.25−0.30	0.0237 ± 0.0093	0.0111 ± 0.0103
0.30−0.35	0.0291 ± 0.0096	-0.0085 ± 0.0108
0.35−0.40	0.0191 ± 0.0100	0.0040 ± 0.0115
0.40−0.50	0.0382 ± 0.0077	-0.0091 ± 0.0090
0.50−0.65	0.0393 ± 0.0073	-0.0172 ± 0.0085
0.65−0.80	0.0483 ± 0.0085	0.0040 ± 0.0097
0.80−1.00	0.0309 ± 0.0084	-0.0094 ± 0.0087

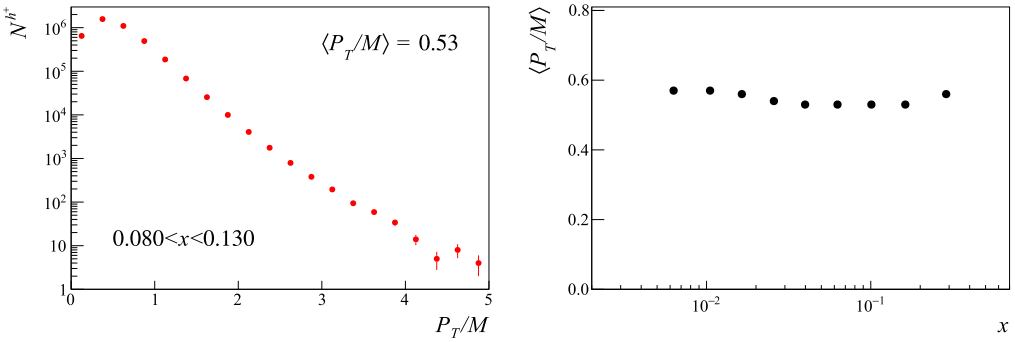

Fig. 6. Left: distribution of the weight $w' = P_T/M$ for positive hadrons in the bin $0.080 < x < 0.13$. Right: mean value of w' as a function of x. No acceptance correction applied.

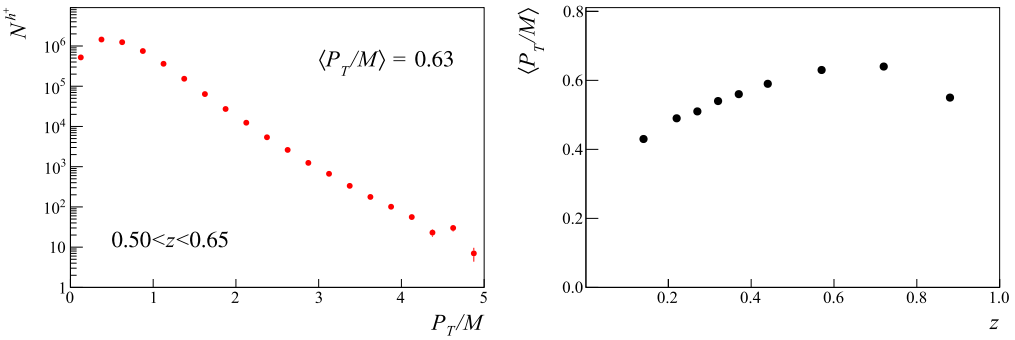

Fig. 7. Left: distribution of the weight $w' = P_T/M$ for positive hadrons in the bin $0.50 < z < 0.65$. Right: mean value of w' as a function of z. No acceptance correction applied.

The results for $A^{w'}_{\rm Siv}$ are shown in Fig. 8 for positive and negative hadrons. The ratio $R^{w'} = A^{w'}_{\rm Siv}/A_{\rm Siv}$ for positive hadrons is shown in Fig. 9. Correlations between numerator and denominator were accounted for. The ratio $R^{w'} = A^{w'}_{\rm Siv}/A_{\rm Siv}$ is almost constant as function of x with a mean value of 0.62, not far from that expected using the Gaussian model [see Eq. (17)], which is also shown in the figure.

Table 4
Mean value of the weight P_T/M for positive hadrons in the nine x bins for $z > 0.2$, and in the nine z bins.

$\langle x \rangle$	$\langle P_T/M \rangle$	$\langle z \rangle$	$\langle P_T/M \rangle$
0.0063	0.57	0.14	0.43
0.0105	0.57	0.22	0.49
0.0164	0.56	0.27	0.51
0.0257	0.54	0.32	0.54
0.0399	0.53	0.37	0.56
0.0629	0.53	0.44	0.59
0.101	0.53	0.57	0.63
0.163	0.53	0.72	0.64
0.288	0.56	0.88	0.55

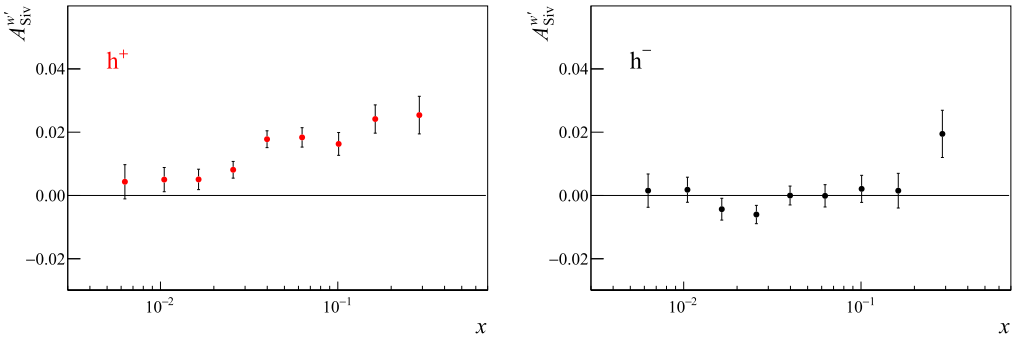

Fig. 8. The weighted asymmetry $A^{w'}_{\mathrm{Siv}}$ with $w' = P^h_T/M$, as a function of x for positive (left) and negative (right) hadrons with $z > 0.2$.

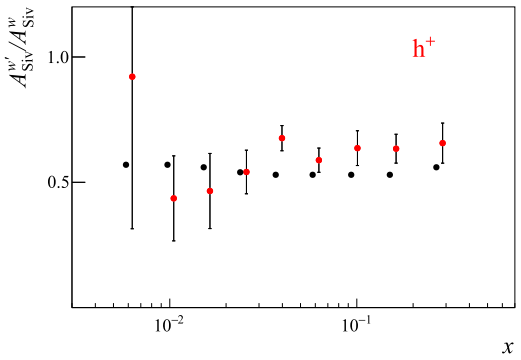

Fig. 9. Ratio $A^{w'}_{\mathrm{Siv}}/A_{\mathrm{Siv}}$ as a function of x for positive hadrons and $z > 0.2$. The black points are the values of $4\langle z \rangle/\pi M \langle z/P_T \rangle$.

In order to better investigate the z dependence, as in the case of the A^{w}_{Siv} asymmetries, the analysis was repeated adding the hadrons with $0.1 < z < 0.2$. The results for the x-integrated asymmetry $A^{w'}_{\mathrm{Siv}}$ as a function of z are shown in Fig. 10 for positive and negative hadrons. The values for positive hadrons are in qualitative agreement with the u-quark dominance approximation, i.e.:

$$A^{w'}_{\mathrm{Siv}}(z) \sim z. \tag{22}$$

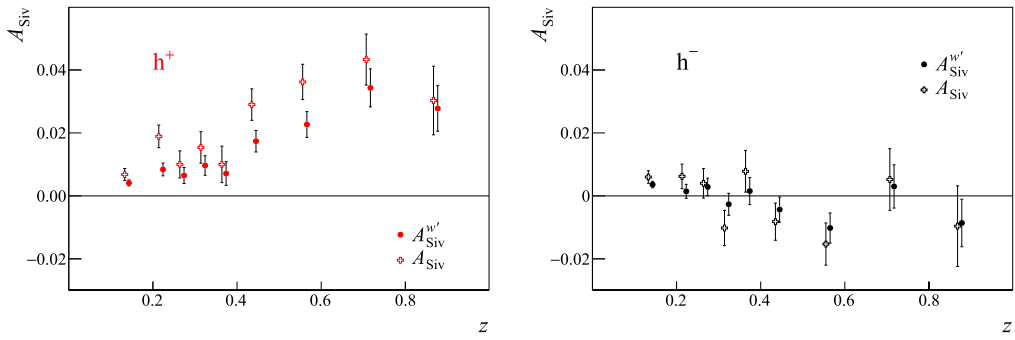

Fig. 10. Closed points: $A_{\mathrm{Siv}}^{w'}$ with $w' = P_T^h/M$ in the nine z bins for positive (left panel) and negative (right panel) hadrons. The open crosses are the unweighted Sivers asymmetries A_{Siv} [11], which are slightly shifted towards smaller x values for clarity.

Table 5
Measured values of the P_T/M-weighted Sivers asymmetries in the nine x bins.

	$z > 0.2$		$0.1 < z < 0.2$	
x	$A_{\mathrm{Siv}}^{w'}$, h^+	$A_{\mathrm{Siv}}^{w'}$, h^-	$A_{\mathrm{Siv}}^{w'}$, h^+	$A_{\mathrm{Siv}}^{w'}$, h^-
0.003−0.008	0.0094 ± 0.0175	0.0034 ± 0.0172	-0.0407 ± 0.0314	0.0007 ± 0.0318
0.008−0.013	0.0135 ± 0.0123	0.0100 ± 0.0129	-0.0096 ± 0.0221	-0.0117 ± 0.0227
0.013−0.020	0.0143 ± 0.0103	-0.0083 ± 0.0112	0.0297 ± 0.0187	0.0217 ± 0.0194
0.020−0.032	0.0212 ± 0.0083	-0.0147 ± 0.0093	0.0496 ± 0.0155	0.0299 ± 0.0162
0.032−0.050	0.0462 ± 0.0083	0.0037 ± 0.0095	0.0246 ± 0.0157	0.0437 ± 0.0168
0.050−0.080	0.0495 ± 0.0094	-0.0016 ± 0.0113	0.0591 ± 0.0180	0.0164 ± 0.0194
0.080−0.130	0.0393 ± 0.0110	0.0100 ± 0.0137	0.0436 ± 0.0212	0.0284 ± 0.0230
0.130−0.210	0.0640 ± 0.0135	0.0074 ± 0.0175	0.0551 ± 0.0264	0.0924 ± 0.0291
0.210−0.700	0.0630 ± 0.0174	0.0701 ± 0.0234	0.0115 ± 0.0343	0.0634 ± 0.0382

Table 6
Measured values of the P_T/M-weighted Sivers asymmetries in the nine z bins.

z	$A_{\mathrm{Siv}}^{w'}$, h^+	$A_{\mathrm{Siv}}^{w'}$, h^-
0.01−0.20	0.0041 ± 0.0010	0.0036 ± 0.0010
0.20−0.25	0.0084 ± 0.0020	0.0015 ± 0.0022
0.25−0.30	0.0065 ± 0.0025	0.0028 ± 0.0028
0.30−0.35	0.0097 ± 0.0031	-0.0027 ± 0.0035
0.35−0.40	0.0071 ± 0.0037	0.0015 ± 0.0043
0.40−0.50	0.0173 ± 0.0034	-0.0044 ± 0.0040
0.50−0.65	0.0227 ± 0.0041	-0.0102 ± 0.0048
0.65−0.80	0.0343 ± 0.0060	0.0030 ± 0.0069
0.80−1.00	0.0278 ± 0.0072	-0.0086 ± 0.0075

For comparison, the published Sivers asymmetries A_{Siv} [11] are also shown in the same figure. All values of the measured P_T/M-weighted asymmetries are given in Tables 5 and 6.[1]

[1] All the numerical values for the results presented in this paper, as well as the covariance matrices are available on HEPDATA [40].

6. Point-by-point extraction of the first moments of the Sivers functions

The final goal of the measurement of the weighted Sivers asymmetries is the extraction of the first moments of the Sivers functions. Thus we consider the weighted asymmetry integrated over z (we restore the Q^2 dependence):

$$A_{\rm Siv}^{w}(x,Q^2) = 2\,\frac{\sum_q e_q^2 x f_{1T}^{\perp\,(1)\,q}(x,Q^2)\,\widetilde{D}_1^q(Q^2)}{\sum_q e_q^2 x f_1^q(x,Q^2)\,\widetilde{D}_1^q(Q^2)}\,, \tag{23}$$

where

$$\widetilde{D}_1^q(Q^2) = \int_{z_{min}}^{z_{max}} {\rm d}z\, D_1^q(z,Q^2)\,. \tag{24}$$

The denominator of Eq. (23) can be fully evaluated by resorting to global fits of distribution and fragmentation functions.

There are two sets of asymmetries, i.e. for unidentified positively (superscript $+$) and negatively (superscript $-$) charged hadrons. In our analysis, we omit the sea-quark Sivers distributions, which were shown to be negligible in a previous study [26]. The asymmetries then read (for simplicity we omit again the x and Q^2 dependence)

$$A_{\rm Siv}^{w,\pm} = 2\,\frac{4 x f_{1T}^{\perp\,(1)\,u_v}\,\widetilde{D}_1^{u,\pm} + x f_{1T}^{\perp\,(1)\,d_v}\,\widetilde{D}_1^{d,\pm}}{9\,\sum_q e_q^2 x f_1^q\,\widetilde{D}_1^{q,\pm}}\,. \tag{25}$$

Denoting the denominator by $\delta^{\pm}$

$$\delta^{\pm} \equiv 9\sum_q e_q^2 x f_1^q\,\widetilde{D}_1^{q,\pm}\,, \tag{26}$$

the valence Sivers distributions can be extracted from the asymmetries as follows

$$x f_{1T}^{\perp\,(1)\,u_v} = \frac{1}{8}\,\frac{\delta^+ A_{\rm Siv}^{w,+}\widetilde{D}_1^{d,-} - \delta^- A_{\rm Siv}^{w,-}\widetilde{D}_1^{d,+}}{\widetilde{D}_1^{u,+}\widetilde{D}_1^{d,-} - \widetilde{D}_1^{d,+}\widetilde{D}_1^{u,-}}\,, \tag{27}$$

$$x f_{1T}^{\perp\,(1)\,d_v} = \frac{1}{2}\,\frac{\delta^- A_{\rm Siv}^{w,-}\widetilde{D}_1^{u,+} - \delta^+ A_{\rm Siv}^{w,+}\widetilde{D}_1^{u,-}}{\widetilde{D}_1^{u,+}\widetilde{D}_1^{d,-} - \widetilde{D}_1^{d,+}\widetilde{D}_1^{u,-}}\,. \tag{28}$$

Eqs. (27) and (28) allow for a point-by-point extraction of the Sivers distributions for valence quarks. For the distribution functions we use the CTEQ5D parametrisation [41] and for the fragmentation functions of unidentified hadrons the DSS parametrisation [42]. The results are displayed in Fig. 11 and tabulated in Table 7 together with the mean values of Q^2 (ranging from 1.24 $({\rm GeV}/c)^2$ to 25.6 $({\rm GeV}/c)^2$). The extracted values for $x f_{1T}^{\perp\,(1)\,u_v}$ and $x f_{1T}^{\perp\,(1)\,d_v}$ are correlated, as they are linear functions of the same two measured asymmetries, and the computed correlation coefficients are also given in Table 7.

The uncertainties are computed from the statistical uncertainties of the measured asymmetries, and no attempt was made to try to assign a systematic uncertainty to the results. The uncertainties in the extracted d_v Sivers distribution are much larger than the corresponding ones for the u_v quark. The u_v and d_v Sivers distributions are linear combinations [see Eqs. (27), (28)] of the same Sivers asymmetries for positive and negative hadrons on the proton, thus in principle sufficient

Table 7
Values of the first moments of the Sivers functions for u and d quarks. The last column gives their correlation coefficient ρ.

$\langle x \rangle$	$\langle Q^2 \rangle$ (GeV/c)^2	$x f_{1T}^{\perp\,(1)\,u_v}$	$x f_{1T}^{\perp\,(1)\,d_v}$	ρ
0.0063	1.27	0.0022 ± 0.0051	-0.001 ± 0.021	-0.26
0.0105	1.55	0.0029 ± 0.0040	0.004 ± 0.017	-0.31
0.0164	1.83	0.0058 ± 0.0037	-0.019 ± 0.015	-0.37
0.0257	2.17	0.0097 ± 0.0033	-0.034 ± 0.013	-0.43
0.0399	2.82	0.0179 ± 0.0036	-0.032 ± 0.015	-0.52
0.0629	4.34	0.0224 ± 0.0046	-0.048 ± 0.019	-0.63
0.101	6.76	0.0171 ± 0.0057	-0.025 ± 0.023	-0.68
0.163	10.6	0.0295 ± 0.0070	-0.056 ± 0.027	-0.65
0.288	20.7	0.0160 ± 0.0073	0.017 ± 0.028	-0.40

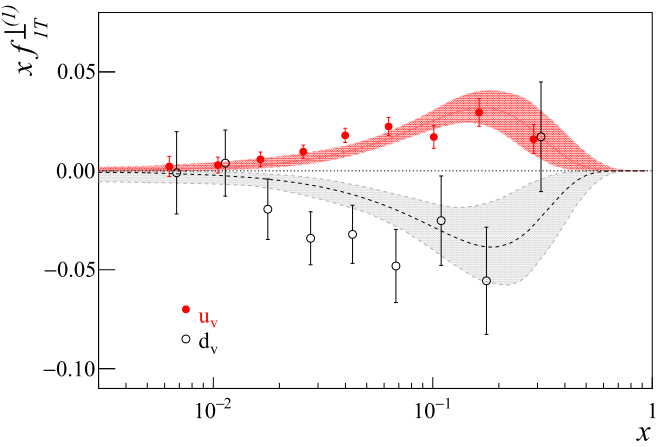

Fig. 11. Values of the first moment of the Sivers function for u (closed red dots) and d (open black dots) quarks from the P_T/zM weighted-Sivers asymmetries for charged hadrons with $z > 0.2$. The curves and the uncertainty bands are the results of the fit of Ref. [23]. (Colours in the figures only in the web version of this article.)

for their determination, but the coefficient of proportionality is four times larger for the d quark, which makes the uncertainties of the extracted $x f_{1T}^{\perp\,(1)\,d_v}$ about four times larger than those of $x f_{1T}^{\perp\,(1)\,u_v}$.

In Fig. 11, we also show for comparison the results, i.e. central values and uncertainty bands, of the fit [23] to the HERMES proton data [9] and the COMPASS proton and deuteron data [38, 43], which uses DGLAP evolution. The results are compatible, with a slightly different trend of $x f_{1T}^{\perp\,(1)\,d_v}$ suggested by the present extraction.

It is also interesting to compare our present result with the point-by-point extraction of Ref. [26], where the pion Sivers asymmetries from the COMPASS proton [38] and deuteron [43] data are used as input. The data set used in Ref. [26] and the present one have the dominating pion data on the proton target in common, so that the results are strongly correlated. As can be seen in Fig. 12, in the present work the uncertainties on the extracted u_v and d_v Sivers function moments are on average smaller by a factor of about 1.5 with respect to the corresponding quantities in Ref. [26]. This is due to the fact that we assumed the Sivers function of the sea quarks to

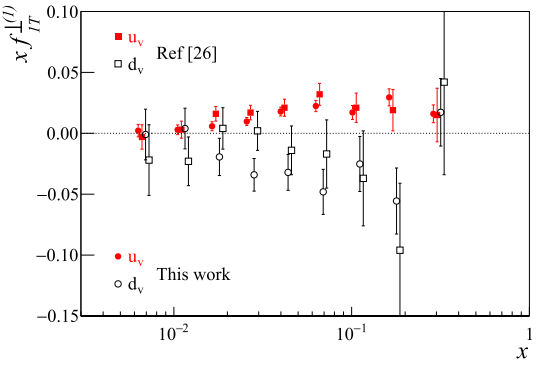

Fig. 12. Comparison of the values of the first moment of the Sivers function for u (closed red dots) and d (open black dots) quarks from the P_T/zM-weighted Sivers asymmetries for charged hadrons with $z > 0.2$, and the corresponding values obtained in Ref. [26] from the unweighted pion Sivers asymmetries measured by COMPASS on deuteron and proton (closed red and open black squares, respectively).

be zero, and no quantitative uncertainty was attributed to this assumption. Following the method of Ref. [26] and imposing the sea-quark Sivers functions to be zero, we have determined the u_v and d_v functions from the π^+ and π^- proton asymmetries [38] only and verified that both the central values and the uncertainties are very similar to the ones presented in this paper. Thus the differences visible in Fig. 12 can be attributed to the impact of the deuteron data and to the extraction of the sea-quark Sivers function, rather then to the use of unweighted asymmetries. The assumption of a vanishing contribution from the sea quarks will be better verified only when more neutron data will be available.

7. Conclusions and outlook

COMPASS has measured the weighted Sivers asymmetries in SIDIS of 160 GeV muons on transversely polarised protons, extending the standard analysis of unweighted asymmetries. These new observables provide the direct access to the first moment of the Sivers function avoiding the transverse-momentum convolution of the TMD Sivers and fragmentation functions, which enter in the standard Sivers asymmetry. The weighted asymmetries were determined for positive and negative hadrons using as weight either P_T/zM or P_T/M. In both cases, the asymmetries were found to be positive for positive hadrons in the range $x > 0.013$ and compatible with zero for negative hadrons with $z > 0.2$, very much as in the case of the standard Sivers asymmetries. The z dependence for positive hadrons agrees with the expectation in the case of u-quark dominance and of a measurement performed in the current-fragmentation region.

From the P_T/zM-weighted Sivers asymmetries, and under the hypothesis of negligible Sivers functions for sea quarks, we have extracted the first moments of the Sivers functions for u_v and d_v quarks. In the leading-order pQCD formalism, the obtained values are model independent because of the use of weighted asymmetries and because of the point-by-point extraction. Extractions of the first moments of the Sivers functions, which are based on the Gaussian ansatz and use the standard proton Sivers asymmetries, compare well with our results.

The present analysis hints at the validity of the Gaussian parametrisation for the transverse-momentum dependence of the Sivers distribution function and the fragmentation function, at least in the kinematic domain explored by our measurement. As in all other extractions of the Sivers functions from SIDIS asymmetries on transversely polarised nucleons, the d-quark Sivers

function turns out to be poorly determined and strongly dependent on the assumptions on the Sivers functions of the sea quarks. This is due to the scarcity of Sivers asymmetry data taken with a transversely polarised deuteron target, as compared to the existing data taken with a transversely polarised proton target. The recently approved COMPASS run [44] with a transversely polarised deuteron target in 2021 is expected to allow for a much better extraction of the Sivers functions for both quarks and antiquarks.

Acknowledgements

We acknowledge the support of the CERN management and staff, as well as the skills and efforts of the technicians of the collaborating institutes. This work was made possible by the financial support of our funding agencies.

Appendix A. Transverse-momentum convolution in the weighted asymmetry

The Sivers asymmetry weighted with the factor $w = P_T/zM$ reads

$$A_{\mathrm{Siv}}^{w}(x,z) = \frac{\sum_q e_q^2 x \int \mathrm{d}^2\boldsymbol{P}_T \, \frac{P_T}{zM} \mathscr{C}\left[\frac{\boldsymbol{P}_T\cdot\boldsymbol{k}_T}{M P_T} f_{1T}^{\perp q}(x,k_T^2)\, D_1^q(z,p_T^2)\right]}{\sum_q e_q^2 x\, f_1^q(x) D_1^q(z)}. \tag{29}$$

The numerator contains the integral

$$\begin{aligned}
&\int \mathrm{d}^2\boldsymbol{P}_T \, \frac{P_T}{zM} \mathscr{C}\left[\frac{\boldsymbol{P}_T\cdot\boldsymbol{k}_T}{M P_T} f_{1T}^{\perp q}\, D_1^q\right] \\
&\quad = \int \mathrm{d}^2\boldsymbol{P}_T \, \frac{P_T}{zM} \int \mathrm{d}^2\boldsymbol{k}_T \int \mathrm{d}^2\boldsymbol{p}_T \, \delta^2(z\boldsymbol{k}_T + \boldsymbol{p}_T - \boldsymbol{P}_T) \, \frac{\boldsymbol{P}_T\cdot\boldsymbol{k}_T}{M P_T} \\
&\quad f_{1T}^{\perp q}(x,k_T^2)\, D_1^q(z,p_T^2)\,.
\end{aligned} \tag{30}$$

Using the delta function to integrate over $\boldsymbol{P}_T$ gives

$$\begin{aligned}
&\int \mathrm{d}^2\boldsymbol{P}_T \, \frac{P_T}{zM} \mathscr{C}\left[\frac{\boldsymbol{P}_T\cdot\boldsymbol{k}_T}{M P_T} f_{1T}^{\perp q}\, D_1^q\right] \\
&\quad = \int \mathrm{d}^2\boldsymbol{k}_T \, \frac{1}{zM^2} \int \mathrm{d}^2\boldsymbol{p}_T \, (z k_T^2 + \boldsymbol{k}_T\cdot\boldsymbol{p}_T)\, f_{1T}^{\perp q}(x,k_T^2)\, D_1^q(z,p_T^2) \\
&\quad = \int \mathrm{d}^2\boldsymbol{k}_T \, \frac{k_T^2}{M^2} f_{1T}^{\perp q}(x,k_T^2) \int \mathrm{d}^2\boldsymbol{p}_T \, D_1^q(z,p_T^2) \\
&\quad = 2\, f_{1T}^{\perp(1)q}(x)\, D_1^q(z)\,.
\end{aligned} \tag{31}$$

References

[1] V. Barone, et al., Prog. Part. Nucl. Phys. 65 (2010) 267.
[2] C.A. Aidala, et al., Rev. Mod. Phys. 85 (2013) 655.
[3] H. Avakian, et al., Eur. Phys. J. A 52 (6) (2016) 150. Erratum: Eur. Phys. J. A 52 (6) (2016) 165.
[4] D.W. Sivers, Phys. Rev. D 41 (1990) 83.
[5] D.W. Sivers, Phys. Rev. D 43 (1991) 261.
[6] S.J. Brodsky, et al., Nucl. Phys. B 642 (2002) 344.
[7] J.C. Collins, Phys. Lett. B 536 (2002) 43.
[8] HERMES Collaboration, A. Airapetian, et al., Phys. Rev. Lett. 94 (2005) 012002.

[9] HERMES Collaboration, A. Airapetian, et al., Phys. Rev. Lett. 103 (2009) 152002.
[10] COMPASS Collaboration, M.G. Alekseev, et al., Phys. Lett. B 692 (2010) 240.
[11] COMPASS Collaboration, C. Adolph, et al., Phys. Lett. B 717 (2012) 383.
[12] COMPASS Collaboration, V.Y. Alexakhin, et al., Phys. Rev. Lett. 94 (2005) 202002.
[13] COMPASS Collaboration, E.S. Ageev, et al., Nucl. Phys. B 765 (2007) 31.
[14] Jefferson Lab Hall A, X. Qian, et al., Phys. Rev. Lett. 107 (2011) 072003.
[15] A.V. Efremov, et al., Phys. Lett. B 568 (2003) 63.
[16] A.V. Efremov, et al., Phys. Lett. B 612 (2005) 233.
[17] J.C. Collins, et al., Phys. Rev. D 73 (2006) 014021.
[18] W. Vogelsang, et al., Phys. Rev. D 72 (2005) 054028.
[19] M. Anselmino, et al., Phys. Rev. D 71 (2005) 074006.
[20] M. Anselmino, et al., Phys. Rev. D 72 (2005) 094007. Erratum: Phys. Rev. D 72 (2005) 099903.
[21] M. Anselmino, Transversity, in: Transversity. Proceedings, Workshop, Como, Italy, September 7–10, 2005, 2005, pp. 9–20.
[22] M. Anselmino, et al., Eur. Phys. J. A 39 (2009) 89.
[23] M. Anselmino, et al., Phys. Rev. D 86 (2012) 014028.
[24] P. Sun, et al., Phys. Rev. D 88 (2013) 034016.
[25] M.G. Echevarria, et al., Phys. Rev. D 89 (2014) 074013.
[26] A. Martin, et al., Phys. Rev. D 95 (9) (2017) 094024.
[27] A.M. Kotzinian, et al., Phys. Rev. D 54 (1996) 1229.
[28] A.M. Kotzinian, et al., Phys. Lett. B 406 (1997) 373.
[29] D. Boer, et al., Phys. Rev. D 57 (1998) 5780.
[30] HERMES Collaboration, I.M. Gregor, Acta Phys. Pol. B 36 (2005) 209.
[31] M. Burkardt, Phys. Rev. D 69 (2004) 091501.
[32] Z.-B. Kang, et al., Phys. Rev. D 87 (3) (2013) 034024.
[33] C. Hadjidakis, et al., arXiv:1807.00603 [/.org/abs].
[34] P.J. Mulders, et al., Nucl. Phys. B 461 (1996) 197.
[35] COMPASS Collaboration, P. Abbon, et al., Nucl. Instrum. Methods A 577 (2007) 455.
[36] COMPASS Collaboration, P. Abbon, et al., Nucl. Instrum. Methods A 779 (2015) 69.
[37] J.H. Koivuniemi, et al., PoS (2015) 015, PSTP2015.
[38] COMPASS Collaboration, C. Adolph, et al., Phys. Lett. B 744 (2015) 250.
[39] COMPASS Collaboration, C. Adolph, et al., Eur. Phys. J. C 77 (4) (2017) 209.
[40] The Durham HepData Project, http://hepdata.cedar.ac.uk/reaction.
[41] H.L. Lai, et al., CTEQ Collaboration, Eur. Phys. J. C 12 (2000) 375.
[42] D. de Florian, et al., Phys. Rev. D 76 (2007) 074033.
[43] COMPASS Collaboration, M. Alekseev, et al., Phys. Lett. B 673 (2009) 127.
[44] COMPASS Collaboration, Addendum to the COMPASS-II Proposal, CERN-SPSC-2017-034 SPSC-P-340-ADD-1 (2018).

The COMPASS Collaboration

M.G. Alexeev [26], G.D. Alexeev [8], A. Amoroso [26,27], V. Andrieux [29,21], N.V. Anfimov [8], V. Anosov [8], A. Antoshkin [8], K. Augsten [8,19], W. Augustyniak [30], C.D.R. Azevedo [2], B. Badełek [31], F. Balestra [26,27], M. Ball [4], J. Barth [5], V. Barone [1,27,ae], R. Beck [4], Y. Bedfer [21], J. Bernhard [13,10], K. Bicker [16,10], E.R. Bielert [10], M. Bodlak [18], P. Bordalo [12,a], F. Bradamante [24,25], A. Bressan [24,25], M. Büchele [9], V.E. Burtsev [28], W.-C. Chang [22], C. Chatterjee [7], M. Chiosso [26,27], A.G. Chumakov [28], S.-U. Chung [16,b], A. Cicuttin [25,c], M.L. Crespo [25,c], S. Dalla Torre [25], S.S. Dasgupta [7], S. Dasgupta [24,25], O.Yu. Denisov [27,*], L. Dhara [7], S.V. Donskov [20], N. Doshita [33], Ch. Dreisbach [16],

W. Dünnweber [d], R.R. Dusaev [28], M. Dziewiecki [32], A. Efremov [8,w], C. Elia [24,25], P.D. Eversheim [4], M. Faessler [d], A. Ferrero [21], M. Finger [18], M. Finger jr. [18], H. Fischer [9], C. Franco [12], N. du Fresne von Hohenesche [13,10], J.M. Friedrich [16,*], V. Frolov [8,10], F. Gautheron [3,29], O.P. Gavrichtchouk [8], S. Gerassimov [15,16], J. Giarra [13], I. Gnesi [26,27], M. Gorzellik [9,r], A. Grasso [26,27], A. Gridin [8], M. Grosse Perdekamp [29], B. Grube [16], A. Guskov [8], D. Hahne [5], G. Hamar [25], D. von Harrach [13], R. Heitz [29], F. Herrmann [9], N. Horikawa [17,h], N. d'Hose [21], C.-Y. Hsieh [22,i], S. Huber [16], S. Ishimoto [33,j], A. Ivanov [26,27], T. Iwata [33], M. Jandek [19], V. Jary [19], R. Joosten [4], P. Jörg [9,g], K. Juraskova [19], E. Kabuß [13], F. Kaspar [16], A. Kerbizi [24,25], B. Ketzer [4], G.V. Khaustov [20], Yu.A. Khokhlov [20,k], Yu. Kisselev [8], F. Klein [5], J.H. Koivuniemi [3,29], V.N. Kolosov [20], K. Kondo [33], I. Konorov [15,16], V.F. Konstantinov [20], A.M. Kotzinian [27,m], O.M. Kouznetsov [8], Z. Kral [19], M. Krämer [16], F. Krinner [16], Z.V. Kroumchtein [8,†], Y. Kulinich [29], F. Kunne [21], K. Kurek [30], R.P. Kurjata [32], A. Kveton [19], A.A. Lednev [20,†], S. Levorato [25], Y.-S. Lian [22,n], J. Lichtenstadt [23], R. Longo [26,27], V.E. Lyubovitskij [28,o], A. Maggiora [27], A. Magnon [29], N. Makins [29], N. Makke [25,c], G.K. Mallot [10], S.A. Mamon [28], B. Marianski [30], A. Martin [24,25], J. Marzec [32], J. Matoušek [24,25,18], T. Matsuda [14], G.V. Meshcheryakov [8], M. Meyer [29,21], W. Meyer [3], Yu.V. Mikhailov [20], M. Mikhasenko [4], E. Mitrofanov [8], N. Mitrofanov [8], Y. Miyachi [33], A. Moretti [24,25], A. Nagaytsev [8], D. Neyret [21], J. Nový [19,10], W.-D. Nowak [13], G. Nukazuka [33], A.S. Nunes [12], A.G. Olshevsky [8], I. Orlov [8], M. Ostrick [13], D. Panzieri [27,p], B. Parsamyan [26,27], S. Paul [16], J.-C. Peng [29], F. Pereira [2], M. Pešek [18], M. Pešková [18], D.V. Peshekhonov [8], N. Pierre [13,21], S. Platchkov [21], J. Pochodzalla [13], V.A. Polyakov [20], J. Pretz [5,l], M. Quaresma [12], C. Quintans [12], S. Ramos [12,a], C. Regali [9], G. Reicherz [3], C. Riedl [29], D.I. Ryabchikov [20,16], A. Rybnikov [8], A. Rychter [32], R. Salac [19], V.D. Samoylenko [20], A. Sandacz [30], S. Sarkar [7], I.A. Savin [8,w], T. Sawada [22], G. Sbrizzai [24,25,*], P. Schiavon [24,25], H. Schmieden [5], E. Seder [21], A. Selyunin [8], L. Silva [12], L. Sinha [7], S. Sirtl [9], M. Slunecka [8], J. Smolik [8], F. Sozzi [25], A. Srnka [6], D. Steffen [10,16], M. Stolarski [12], O. Subrt [10,19], M. Sulc [11], H. Suzuki [33,h], A. Szabelski [24,25,30], T. Szameitat [9,r], P. Sznajder [30], M. Tasevsky [8], S. Tessaro [25], F. Tessarotto [25], A. Thiel [4], J. Tomsa [18], F. Tosello [27], V. Tskhay [15],

S. Uhl [16], B.I. Vasilishin [28], A. Vauth [10], B.M. Veit [13], J. Veloso [2], A. Vidon [21], M. Virius [19], M. Wagner [4], S. Wallner [16], M. Wilfert [13], K. Zaremba [32], P. Zavada [8], M. Zavertyaev [15], Y. Zhao [25], E. Zemlyanichkina [8,w], M. Ziembicki [32]

[1] *Universita' degli Studi del Piemonte Orientale "A. Avogadro", Di.S.I.T., 15121 Alessandria, Italy*
[2] *University of Aveiro, Dept. of Physics, 3810-193 Aveiro, Portugal*
[3] *Universität Bochum, Institut für Experimentalphysik, 44780 Bochum, Germany* [s,t]
[4] *Universität Bonn, Helmholtz-Institut für Strahlen- und Kernphysik, 53115 Bonn, Germany* [s]
[5] *Universität Bonn, Physikalisches Institut, 53115 Bonn, Germany* [s]
[6] *Institute of Scientific Instruments, AS CR, 61264 Brno, Czech Republic* [u]
[7] *Matrivani Institute of Experimental Research & Education, Calcutta-700 030, India* [v]
[8] *Joint Institute for Nuclear Research, 141980 Dubna, Moscow region, Russia* [w]
[9] *Universität Freiburg, Physikalisches Institut, 79104 Freiburg, Germany* [s,t]
[10] *CERN, 1211 Geneva 23, Switzerland*
[11] *Technical University in Liberec, 46117 Liberec, Czech Republic* [u]
[12] *LIP, 1000-149 Lisbon, Portugal* [x]
[13] *Universität Mainz, Institut für Kernphysik, 55099 Mainz, Germany* [s]
[14] *University of Miyazaki, Miyazaki 889-2192, Japan* [y]
[15] *Lebedev Physical Institute, 119991 Moscow, Russia*
[16] *Technische Universität München, Physik Dept., 85748 Garching, Germany* [s,d]
[17] *Nagoya University, 464 Nagoya, Japan* [y]
[18] *Charles University in Prague, Faculty of Mathematics and Physics, 18000 Prague, Czech Republic* [u]
[19] *Czech Technical University in Prague, 16636 Prague, Czech Republic* [u]
[20] *State Scientific Center Institute for High Energy Physics of National Research Center 'Kurchatov Institute', 142281 Protvino, Russia*
[21] *IRFU, CEA, Université Paris-Saclay, 91191 Gif-sur-Yvette, France* [t]
[22] *Academia Sinica, Institute of Physics, Taipei 11529, Taiwan* [z]
[23] *Tel Aviv University, School of Physics and Astronomy, 69978 Tel Aviv, Israel* [aa]
[24] *University of Trieste, Dept. of Physics, 34127 Trieste, Italy*
[25] *Trieste Section of INFN, 34127 Trieste, Italy*
[26] *University of Turin, Dept. of Physics, 10125 Turin, Italy*
[27] *Torino Section of INFN, 10125 Turin, Italy*
[28] *Tomsk Polytechnic University, 634050 Tomsk, Russia* [ab]
[29] *University of Illinois at Urbana-Champaign, Dept. of Physics, Urbana, IL 61801-3080, USA* [ac]
[30] *National Centre for Nuclear Research, 00-681 Warsaw, Poland* [ad]
[31] *University of Warsaw, Faculty of Physics, 02-093 Warsaw, Poland* [ad]
[32] *Warsaw University of Technology, Institute of Radioelectronics, 00-665 Warsaw, Poland* [ad]
[33] *Yamagata University, Yamagata 992-8510, Japan* [y]

[*] Corresponding authors.
E-mail addresses: oleg.denisov@cern.ch (O.Yu. Denisov), jan.friedrich@cern.ch (J.M. Friedrich), giulio.sbrizzai@ts.infn.it (G. Sbrizzai).

[a] Also at Instituto Superior Técnico, Universidade de Lisboa, Lisbon, Portugal.

[b] Also at Dept. of Physics, Pusan National University, Busan 609-735, Republic of Korea and at Physics Dept., Brookhaven National Laboratory, Upton, NY 11973, USA.

[c] Also at Abdus Salam ICTP, 34151 Trieste, Italy.

[d] Supported by the DFG cluster of excellence 'Origin and Structure of the Universe' (www.universe-cluster.de) (Germany).

[e] Supported by the Laboratoire d'excellence P2IO (France).

[f] Present address: University of Connecticut, Storrs, Connecticut 06269, US.

[g] Present address: Universität Bonn, Physikalisches Institut, 53115 Bonn, Germany.

[h] Also at Chubu University, Kasugai, Aichi 487-8501, Japan[y].

[i] Also at Dept. of Physics, National Central University, 300 Jhongda Road, Jhongli 32001, Taiwan.
[j] Also at KEK, 1-1 Oho, Tsukuba, Ibaraki 305-0801, Japan.
[k] Also at Moscow Institute of Physics and Technology, Moscow Region, 141700, Russia.
[l] Present address: RWTH Aachen University, III. Physikalisches Institut, 52056 Aachen, Germany.
[m] Also at Yerevan Physics Institute, Alikhanian Br. Street, Yerevan, 0036, Armenia.
[n] Also at Dept. of Physics, National Kaohsiung Normal University, Kaohsiung County 824, Taiwan.
[o] Also at Institut für Theoretische Physik, Universität Tübingen, 72076 Tübingen, Germany.
[p] Also at University of Eastern Piedmont, 15100 Alessandria, Italy.
[q] Present address: Uppsala University, Box 516, 75120 Uppsala, Sweden.
[r] Supported by the DFG Research Training Group Programmes 1102 and 2044 (Germany).
[s] Supported by BMBF – Bundesministerium für Bildung und Forschung (Germany).
[t] Supported by FP7, HadronPhysics3, Grant 283286 (European Union).
[u] Supported by MEYS, Grant LG13031 (Czech Republic).
[v] Supported by B. Sen fund (India).
[w] Supported by CERN-RFBR Grant 12-02-91500.
[x] Supported by FCT – Fundação para a Ciência e Tecnologia, COMPETE and QREN, Grants CERN/FP 116376/2010, 123600/2011 and CERN/FIS-NUC/0017/2015 (Portugal).
[y] Supported by MEXT and JSPS, Grants 18002006, 20540299, 18540281 and 26247032, the Daiko and Yamada Foundations (Japan).
[z] Supported by the Ministry of Science and Technology (Taiwan).
[aa] Supported by the Israel Academy of Sciences and Humanities (Israel).
[ab] Supported by the Russian Federation program “Nauka” (Contract No. 0.1764.GZB.2017) (Russia).
[ac] Supported by the National Science Foundation, Grant no. PHY-1506416 (USA).
[ad] Supported by NCN, Grant 2017/26/M/ST2/00498 (Poland).
[ae] Partially supported by “Fondi Ricerca Locale ex 60%” Universita’ del Piemonte Orientale (Italy).
[†] Deceased.